ELSEVIER

FEBS Letters 343 (1994) 261–266

FEBS 13958

FEBS LETTERS

NMR structures of ferredoxin chloroplastic transit peptide from *Chlamydomonas reinhardtii* promoted by trifluoroethanol in aqueous solution

Jean-Marc Lancelin[a,*], Isabelle Bally[a], Gérard J. Arlaud[a], Martin Blackledge[a], Pierre Gans[a], Mariana Stein[b], Jean-Pierre Jacquot[b]

[a]*Institut de Biologie Structurale CEA-CNRS, 41, Avenue des Martyrs, F-38027 Grenoble cedex, France*
[b]*Laboratoire de Physiologie Végétale Moléculaire, Bâtiment 430, Unité Associée au CNRS 1128, Université de Paris-Sud, F-91405 Orsay, France*

Received 7 March 1994

Abstract

The 32-amino acid transit peptide of the unicellular green alga *Chlamydomonas reinhardtii* ferredoxin has been synthesized and analysed by NMR spectroscopy and circular dichroism. The results show that while the peptide is unstructured in water, it undergoes an α-helix formation from residue 3 to 13 in a 30:70 molar-ratio mixture of 2,2,2-trifluoroethanol. The remainder of the peptide is still unstructured in CF_3CD_2OD/H_2O mixtures, but is distributed on a side opposite to a hydrophobic ridge formed by Met^5, Phe^9 and Val^{13} on the induced α-helix. The NMR structures driven by 2,2,2-trifluoroethanol in aqueous solution, are discussed in terms of potent interactions with the chloroplast envelope and its translocation molecular machinery.

Key words: Chloroplast protein import; Transit peptide; Ferredoxin; Petide synthesis; NMR structure; *Chlamydomonas reinhardtii*

1. Introduction

Nuclear encoded chloroplastic proteins are synthesized in the cytosol and have to be post-translationally and selectively routed to the chloroplast. A pioneer work on the small subunit of ribulose biphosphate carboxylase [1], showed that an N-terminal peptidic extension to the mature protein is required for triggering the ATP-dependent translocation mechanism through the chloroplastic envelope to the stroma where the peptidic transit sequence is cleaved off (for reviews see [2,3]).

Several transit sequences have been identified in the past five years from very different photosynthetic eukaryotes ranging from higher plants to unicellular algae. Since no consensus sequence has ever been convincingly identified between transit peptides, the possibility of a common conformational behaviour, presumably important for the function of the transit sequence, was proposed several times [2–4]. Very recently, the 47-amino acid ferredoxin transit peptide from *Silene pratensis* was reported to possess a secondary structure that can be modulated from a random coil conformation in water to a ca. 50% helical structure, either by addition of 2,2,2-trifluoroethanol (TFE) [5] or in the presence of lipidic micelles of particular compositions [6]. The location of the induced helical structure, is, however, unknown.

A cDNA clone coding for the green alga *Chlamydomonas reinhartii* preferredoxin has been sequenced [7], revealing a typical transit sequence made of 32 amino acids with no apparent homologies to the one of *S. pratensis* ferredoxin. In order to gain a better molecular understanding of protein import in relation to the structure of chloroplastic transit peptides (cTP), we prepared the *C. reinhartii* ferredoxin cTP by solid-phase peptide synthesis and analysed it by CD and NMR spectroscopy either in water or in water/TFE mixtures that mimic the CD-observed effects exerted by negatively charged lipids on the unrelated *S. pratensis* ferredoxin cTP [6]. We calculated structures of *C. reinhartii* ferredoxin cTP based on 186 geometric boundaries, derived from NMR data in 36% H_2O/64% CF_3CD_2OD at 10°C, by a simulated annealing-restrained molecular dynamic (rMD) protocol starting from a random array of atoms. The structures obtained are discussed in terms of potent interactions with the chloroplastic envelope and the molecular translocation machinery.

*Corresponding author. Fax: (33) 76885494.
E-mail: lancelin@rmn.ibs.fr

Abbreviations: cTP, chloroplastic transit peptide; CD, circular dichroism; TFE, 2,2,2-trifluoroethanol; rMD, restrained molecular dynamic; R.m.s., root-mean-square; R.m.s.d., R.m.s. deviation.

SSDI 0014-5793(94)00343-T

2. Materials and methods

2.1. Peptide synthesis

The ferredoxin cTP was synthesized chemically by the stepwise solid-phase method [9], using an Applied Biosystems 430A automated synthesizer. The *tert*-butyloxycarbonyl group was used for protection of the *N*-α-amino terminus of all amino acids, and synthesis was carried out on a phenylacetamidomethyl-resin. Protecting groups for amino acid side chains were the following: Arg (mesitylene sulfonyl), Cys (4-methoxybenzyl), Lys (2-chlorobenzyl oxycarbonyl), Ser (benzyl), Thr (benzyl). Met was used without side-chain protection. All couplings were performed by the dicyclohexylcarbodiimide/1-hydroxybenzotriazole method, using *N*-methyl pyrrolidone and dimethylsulfoxide as coupling solvents, according to the protocol recommended by Applied Biosystems. All amino acids, except Gly, were double coupled, and amino groups left unreacted at the end of each coupling cycle were capped with acetic anhydride.

Deprotection and cleavage of the peptide from the resin was achieved by HF treatment [9]. Reduction of methionine sulfoxide generated during synthesis was performed by treatment of the peptide with *N*-methyl mercaptoacetamide, as described previously [10]. Purification of the peptide was achieved by preparative reverse-phase HPLC on a 30-nm Vydac C18 column (2.2 cm × 25 cm, 10 μm). Fractions of 50–100 mg of the peptide, in 6 M guanidine hydrochloride, were first loaded onto the column equilibrated with solvent system 1, consisting of 0.1% trifluoroacetic acid and CH_3CN in the ratio 95:5 (v/v), and elution was carried out with a 30-min linear gradient to give a final ratio of 40:60. Further purification was achieved on the same column using a second solvent system containing 0.1% triethylammonium phosphate, using a 30-min linear gradient from 5 to 40% CH_3CN. Desalting of the peptide was realized by a final chromatographic step using solvent system 1. Analytical separations were performed on a 30-nm Vydac C18 column (0.46 cm × 25 cm, 5 μm) using solvent system 1. The peptide was detected by its absorption at 215 nm.

2.2. Fast-atom-bombardment mass spectrometry

The peptide was dissolved in 0.1% trifluoroacetic acid containing 10% CH_3CN and the matrix used was thioglycerol: glycerol 1:1. Spectra were recorded on a VG analytical ZAB-SE double-focussing mass spectrometer as described previously [11].

2.3. Circular dichroism

Spectra were recorded at 10°C and 25°C between 190 and 250 nm on a Jobin-Yvon CD6 spectro-dichrograph, using a quartz cell of 1 mm path length, with a 5 s integration time of each 0.5 nm step. For each condition, two spectra were averaged and the baseline was corrected for neat solvents or solvent mixtures. Water-TFE mixtures were obtained by mixing two equivalent solutions of ferredoxin cTP at 110 μg/ml, prepared either in pure bi-distillated water (pH 3.7) or in TFE (Aldrich Chemicals Co.).

2.4. NMR measurements

Samples were dissolved at a 5 mM concentration in 90% H_2O/10% ^2H_2O and the pH adjusted to 4.0 at 25°C (direct uncorrected pH-meter reading) by addition of μl increments of 0.1 N NaOH and 0.1 N HCl. A sample in 36% H_2O/64% CF_3CD_2OD (70:30, mol/mol) was obtained from the lyophilisation of a sample in 90% H_2O/10% ^2H_2O (pH 4.0), followed by dissolution in the H_2O/CF_3CD_2OD solvent mixture. In both cases, samples were sealed in a 5 mm diameter NMR tube under Argon.

NMR spectra were recorded on Bruker AM-X spectrometers operating at 400 MHz and 600 MHz proton frequencies, at 25°C and 10°C, respectively. Chemical shifts were quoted relative to the water resonance fixed at 4.77 ppm at 25°C and at 4.92 ppm at 10°C. ^1H 2D spectra, DQF-COSY (double quantum filtered correlation spectroscopy) [12], TOCSY/HOHAHA (total correlation spectroscopy/homonuclear Hartmann-Hahn spectroscopy) [13,14], and NOESY (nuclear Overhauser spectroscopy) [15,16] spectra were recorded in the phase sensitive mode using the hypercomplex method [17]. Water resonance was attenuated by means of a coherent low-power (γB_2 = 50 Hz) presaturation during the relaxation delay. For HOHAHA and NOESY this presaturation was further combined with a 'jump and return' read pulse [18]. The Waltz-17 mixing scheme used in TOCSY/HOHAHA experiments was optimized according to the technique known as clean TOCSY [19]. Two-dimensional spectra were collected as 512 (t_1) and 1,024 (t_2) complex point time-domain matrix with a spectral width of 3,400 Hz (^1H = 400 MHz) or 5,100 Hz (^1H = 600 MHz) in both dimensions and 32 scans per t_1 increment. They were transformed after zero-filling in the *F*1 dimension, into 1,024 and 1,024 real points in *F*1 and *F*2 dimension frequency-domain spectra. HOHAHA spectra were recorded with a mixing time of 45 ms that includes the delays of the clean-TOCSY pulse scheme. NOESY spectra were recorded with a 300-ms mixing time.

2.5. NMR-derived geometrical bounds

From the NOESY spectrum recorded in 36% H_2O/64% CF_3CD_2OD at 10°C, the relative intensities of NOE cross-peaks were converted as 2.7, 3.3, and 5.0 Å upper-distance boundaries for a strong, medium and weak intensities, respectively. 0.3 Å was added to a distance boundary involving an amide proton. The possibility of spin diffusion precludes higher precision in the derivation of distance limits. Methyl, methylene, and aromatic protons that give rise to a single resonance line were treated as a pseudo-atom at their geometric center and the distances were corrected according to the pseudo-structure generated [20]. All other methylene protons were treated individually as floating prochiral pairs. A φ dihedral restraint was applied when a $^3J_{HN\alpha}$ was measured smaller than 5 Hz (−65° ± 25) or greater than 8 Hz (−120° ± 40).

2.6. Structure calculations

Structural calculations were performed using the molecular dynamics program DISCOVER (version 2.9) from Biosym Technologies with the AMBER force field [21]. The protocol was divided into two parts: in the first stage a simulated annealing procedure was used to provide the broadest possible sampling of the conformational space. Cartesian coordinates were randomised at the start of each run. In the initial stages the calculation is dominated by the experimental distances (force constant for the semi-parabolic distance constraints was 50 $kcal \cdot mol^{-1} \cdot Å^{-2}$); experimental, covalent and non-bond terms were augmented gradually during the high-temperature (1,000 K) period of the simulation before final cooling to 300 K [22]. The non-bond terms were reduced to a simple repulsive quartic term to facilitate interrogation of a large conformational space and the coulombic interaction was ignored in this first step. Total simulation time in this first step was 62 ps. These approximate structures were then refined using a rMD calculation using the full AMBER force field description (including Coulomb and van der Waals terms). Solvent effects were approximated using reduced charges for the polar residues and a distance dependant dielectric term. The molecule was equilibrated at a temperature of 600 K, using distance constraints of 25 $kcal \cdot mol^{-1} \cdot Å^{-2}$, allowed to evolve during a period of 10 ps and then cooled over a period of 5 ps to 300 K, where the molecule was again allowed to evolve over 15 ps. Step size for the calculation of velocities was 1 fs. Final structures were energy minimised using the same force field with a conjugate gradient algorithm and these structures used for analysis.

3. Results

Chromatographic analysis of the final synthetic product by analytical reverse-phase HPLC indicated that it was more than 95% pure. FAB-mass-spectrometry analysis indicated that the peptide had the expected sequence, yielding an *m/z* value of 3,342.8, corresponding to the ($M + H^+$) pseudo-molecular ion (calculated molecular mass = 3,343.1).

The NMR sequence-specific proton assignment [20] of ferredoxin cTP was obtained in a straightforward manner either in 90% H_2O/10% ^2H_2O at pH 4.0 or in 36% H_2O/64% CF_3CD_2OD at 10°C. A temperature of 10°C was found to be useful for the sample in 90% H_2O/10% ^2H_2O to restore a molecular motional regim compatible with large negative NOE effects, since only very weak

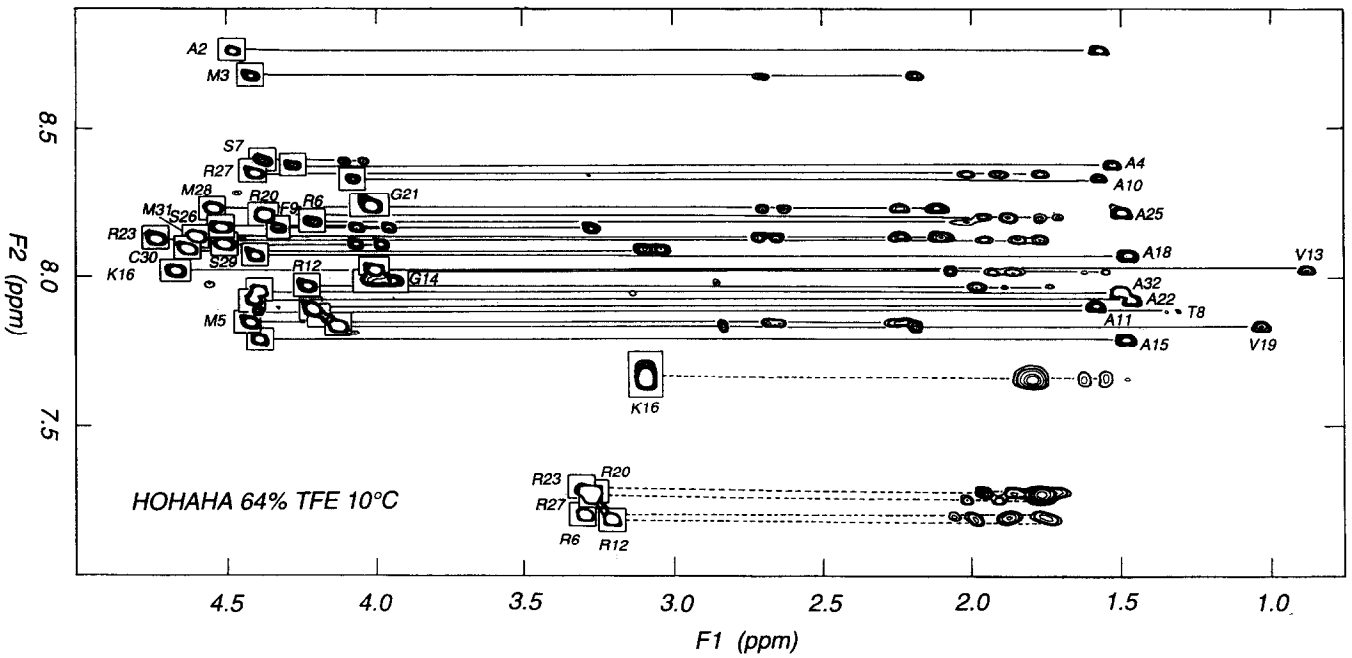

Fig. 1. NH(F_2)-aliphatic(F_1) region of the HOHAHA spectrum recorded at 600 MHz (45 ms of mixing time) of synthetic *C. reinhardtii* ferredoxin cTP 5 mM in 36% H_2O/64% CF_3CD_2OD at 10°C. Spin systems are connected from the (NH, $C^{\alpha}H$) cross-peaks (boxes). Dotted lines indicates additional magnetisation transferts that arise from $N^{\delta}H$ and $N^{\epsilon}H$ of Arg and Lys, respectively.

NOEs were detected at 25°C. Fig. 1 and Fig. 2, respectively, show representative parts of the HOHAHA and NOESY spectra in 36% H_2O/64% CF_3CD_2OD, and the overall quality of the NMR spectra.

The systematic search for medium and long-distance NOEs as well as the observation of spin-spin coupling constants $^3J_{HN\alpha}$, combined with a careful consideration of the relative intensities of the $d_{\alpha N}$ vs. d_{NN} NOE cross-peaks as shown in Fig. 3, led to the following qualitative conformational assignment: (i) the peptide is mainly un-

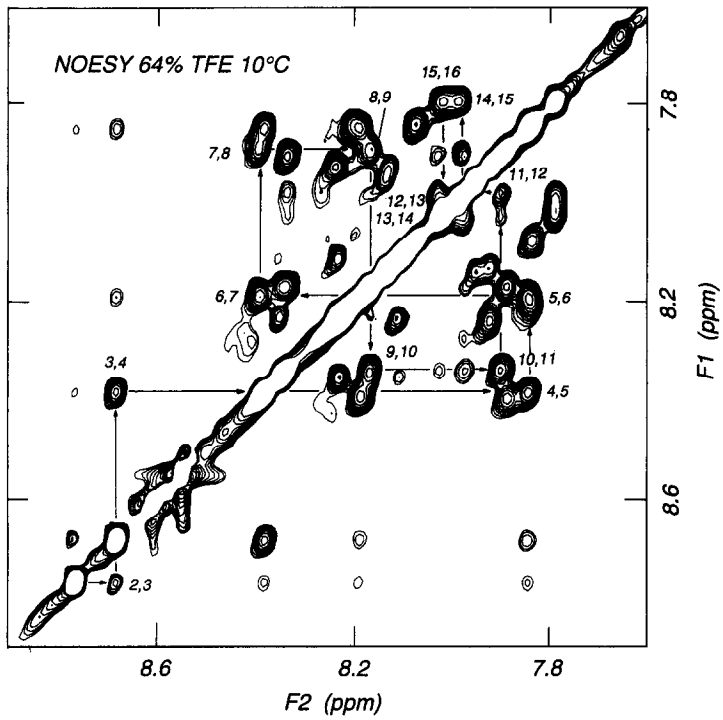

Fig. 2. NH(F_2)-NH(F_1) region of the NOESY spectrum recorded at 600 MHz (300 ms of mixing time) of synthetic *C. reinhardtii* ferredoxin cTP, 5 mM in 36% H_2O/64% CF_3CD_2OD at 10°C. Sequential connectivities are arrowed from Ala^2 to Arg^{16}.

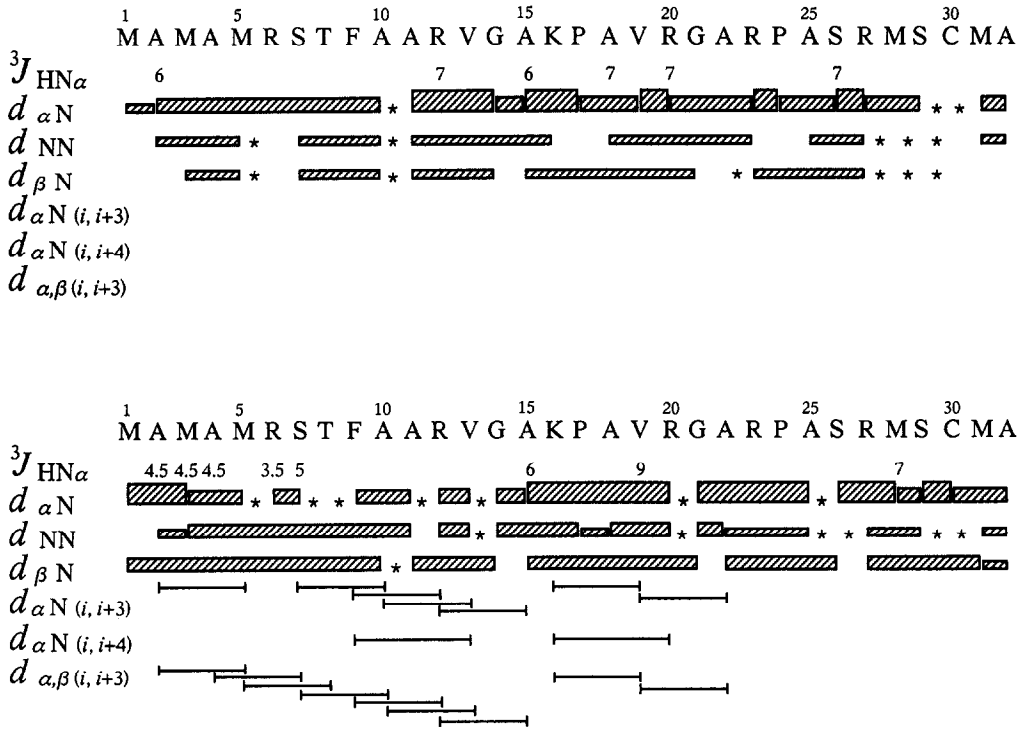

Fig. 3. Summary of the sequential NOE connectivities involving NH, $C^{\alpha}H$ and $C^{\beta}H$ measured at 10°C and 300 ms mixing time. NOEs are classified as strong, medium and weak according to the height of the hatched bar under the peptidic sequence. The upper-trace represents the NOEs measured in 90% H_2O/10% ^2H_2O at at pH 4.0 and 10°C. The lower-trace represents the NOEs measured in 36% H_2O/64% CF_3CD_2OD at the same temperature. For Pro^{17} and Pro^{23} NOEs with $C^{\delta}H$ instead of NH are indicated. Asterisks indicate a spectral overlap that precludes the observation of the NOE. Spin-spin coupling constants $^3J_{HN\alpha}$ (expressed in Hz) were measured on one dimensional spectra at 25°C.

structured in 90% H_2O/10% ^2H_2O; (ii) in 36% H_2O/64% CF_3CD_2OD, it undergoes an helix formation starting from Met^3 that stops around Gly^{14}; (iii) the intensity ratio between $d_{\alpha N}$ and d_{NN} (i.e. strong vs. medium), as well the value of the $^3J_{HN\alpha}$ for Ala^{15} and Val^{19}, preclude a stable extent of this helix formation beyond Gly^{14}, even though medium distance NOEs were observed between Lys^{16} and Val^{19}, or Val^{19} and Ala^{21}; (iv) Pro^{17} and Pro^{23} are in a *trans* peptidic conformation at the NMR time scale, as indicated by the sequential $d_{\alpha\delta}$ in Fig. 3.

These qualitative conformational NMR assignments were validated by a series of CD measurements by recording the far-UV spectra of the *C. reinhardtii* ferredoxin cTP in water and in water-TFE mixtures as shown in Fig. 4. The 10 and 25°C spectra in water exhibit a profile that is typical of a random-coil conformation with a quasi-zero mean residue ellipticity at 222 nm, that characterises the absence of helix content. When increasing the amount of TFE, the spectrum exhibits increasing helical contribution with an isodichroic point around 203 nm, indicative of a two-state coil-to-helix transition. At 65% TFE in water, the mean-residue ellipticity at 222 nm reached ca. −10,000 deg·cm^2·dmol^{-1} at 10°C which corresponds to approximately one-third of the 32 amino acids in helical conformation. Only a slight increase of this value to ca. −9,500 deg·cm^2·dmol^{-1} was observed at 25°C.

From the NOESY spectrum, we derived an ensemble of 186 geometrical boundaries that comprises 6 φ dihedral-angle restraints, 133 sequential and 46 medium-range upper-bound distances. No intra-residue distance restraints were used as an input data in the structure calculation procedure. Fig. 5 shows 27 structures that fulfil the common structural quality criteria as described in Table 1. Of the 32 calculations performed, 5 structures were rejected on the basis of a non-bond energy threshhold at the end of the restrained molecular dynamics calculation. Most of the structures present a regular α-helix conformation from residue 3 to 13 and are especially well-defined starting from residue 5 (Fig. 5, Table 1). Conversely, a pronounced disorder occurs from Gly^{14} until the C-terminal end. As shown in Table 1, almost all of the residual violations of the experimental restraints are located in this disordered region.

4. Discussion

We have shown by both NMR and CD that the isolated *C. reinhardtii* ferredoxin cTP possesses, as described for the one of *S. pratensis* [6], an intrinsic conformational flexibility that can drive the peptide structure from a random coil in water to a helical conformation in water/TFE mixtures. In addition, we have demon-

strated that this helical structure is limited to the N-terminal 3–13 region of the *C. reinhardtii* ferredoxin cTP. The effect of TFE on peptides in aqueous solution, though known since a long time, is still unclear regarding the precise mechanism of its α-helix promotion property [23].

The α-helix formed, contains an hydrophobic ridge aligned along its axis that includes the side chains of Met^5, Phe^9 and Val^{13} as shown in Fig. 5. Similar to most of the cTPs, the structure does not contain any acidic amino acids and is heavily positively charged at physiological pH. Including the N-terminal amino group of Met1, *C. reinhardtii* ferredoxin cTP possesses 7 cationic groups with one arginine located next to the beginning (Arg^6) and one near the end (Arg^{12}) of the α-helix promoted in water/TFE mixtures. The other cationic groups (Lys^{16}, Arg^{20}, Arg^{23}, Arg^{27}) are then located on the C-terminal unstructured region, spaced by 2–4 amino acids. From Fig. 5 it is clear that this latter region is distributed on the opposite side to the hydrophobic ridge. This can be attributed, in particular, to medium-distance restraints between C^α and C^β protons of Arg^{12} located in the well-defined α-helix, and Ala^{15} located in the disordered region of the models, that participate to give a global orientation of the second half of the peptide relative to the α-helix.

The TFE-driven structures of the *C. reinhardtii* ferredoxin cTP suggests several hypotheses concerning its role in the chloroplast protein import. First, the possibility of forming the above-described α-helix, would provide a preliminary anchor to the chloroplast membrane surface by a specific interaction of both Arg^6 and Arg^{12} with negatively-charged polar heads of phospholipids, while the hydrophobic ridge comprising the side chains of Met^5, Phe^9 and Val^{13} would penetrate the surface to optimise hydrophobic contacts. On the other hand, the particular resistance to the structuration of the second

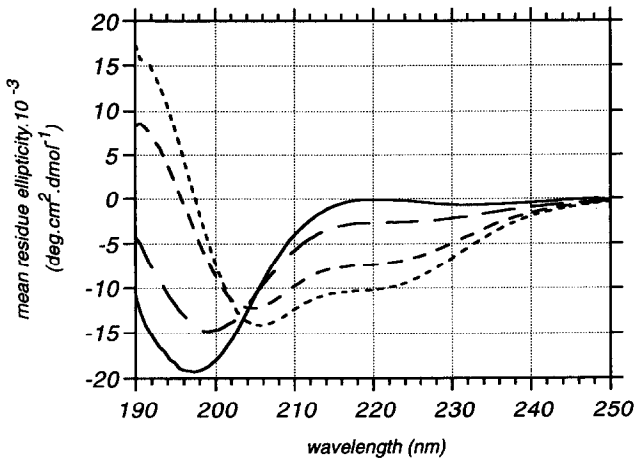

Fig. 4. CD spectra of *C. reinhardtii* ferredoxin cTP at 10°C: (1) in water at pH 3.7; (2) in 80% H_2O/20% CF_3CH_2OH; (3) in 60% H_2O/40% CF_3CH_2OH; (4) in 35% H_2O/65% CF_3CH_2OH.

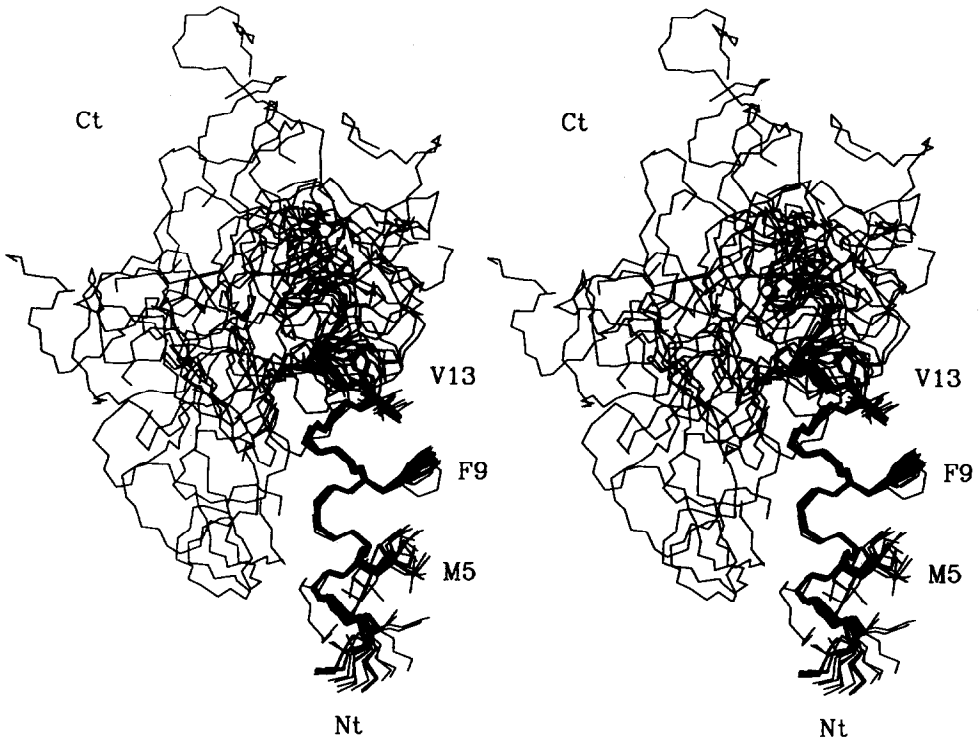

Fig. 5. R.m.s. superpositions of (N, C^α, C) atoms of residue 4 to 13 of 27 calculated structures of *C. reinhardtii* ferredoxin cTP with geometrical boundaries derived from the NMR experiments at 10°C in 36% H_2O/64% CF_3CD_2OD. In addition to (N, C^α, C) atoms, heavy atoms of the side chains from Met^5, Phe^9 and Val^{13} are represented. For the sake of clarity, segments comprizing residues 15 to 32 of two structures have been omitted. Nt = N-terminal ends; Ct = C-terminal ends.

Table 1
Structural statistics for the 27 structures of *C. reinhardtii* ferredoxin cTP in 36% H_2O/64% CF_3CD_2OD*.

Structural statistics	27 structures
Cartesian coordinate R.m.s.d. (Å)**	
Residues 3 to 14	0.29 ± 0.29
Residues 5 to 14	0.22 ± 0.11
Mean number of distance restraints violation per structure	
> 0.4 Å	0
> 0.3 Å	1.9 ± 0.1
> 0.2 Å	4.9 ± 1.4
> 0.1 Å	10.9 ± 2.3
Mean number of distance restraints violation per structure in residues 3 to 14	
> 0.4 Å	0
> 0.3 Å	0.15 ± 0.35
> 0.2 Å	0.30 ± 0.45
> 0.1 Å	0.93 ± 0.77
AMBER potential energies***	
F_{TOTAL} (kcal·mol^{-1})	−407 ± 14
$F_{COULOMBIC}$ (kcal·mol^{-1})	−444 ± 13
E_{L-J} (kcal·mol^{-1})	− 42 ± 7

*The '27 structures' refer to the final NMR-derived structures.
**Mean R.m.s.d were calculated vs. the averaged coordinates of the 27 structures using (N, C^{α}, C) backbone atoms.
*** $F_{COULOMBIC}$ is the coulombic energy contribution to F_{TOTAL}. E_{L-J} is the value of the Lennard–Jones van der Waals energy function calculated by DISCOVER using the AMBER force-field [21].

half of the peptide, could be interpreted as a favorable phenomenon to keep it exposed and available for a putative interaction with membrane proteins of the ATP-dependent translocation molecular machinery of the chloroplast. Then, the selective targeting to the chloroplast could reside either on a preferential primary interaction of the induced α-helix with the inner-membrane of the envelope which, itself, presents a specific lipidic composition, and/or the selective interaction of the unstructured domain with the envelope proteins responsible of later processes of the translocation.

From the fact that the known cTP from *C. reinhardtii* are usually shorter, and do not present obvious sequence homologies to those of higher plants such as *S. pratensis* [24], the question arises whether the observed effect on *C. reinhardtii* ferredoxin cTP is general within the plant kingdom or not. If so, we could propose a broad amino acid sequence requirement for such a conformational property.

Acknowledgements: Coordinates have been deposited at the Protein Data Bank at Broohaven National Laboratory. We thank Biosym Inc. (San Diego, CA, USA) for the generous gift of their ensemble of molecular modeling programs. Finally, the authors thank Dr. M. Miginiac-Maslow for critical reading of the manuscript.

References

[1] Dobberstein, B., Blobel, G. and Chua, N.-H. (1977) Proc. Natl. Acad. Sci. USA 74, 1082–1085.
[2] Douwne de Boer, A. and Weisbeck P.J. (1991) Biophys. Biochim. Acta 1071, 221–253.
[3] Keegstra, K. (1989) Cell 56, 247–253.
[4] von Heijne, G., Steppuhn, J. and Herrmann, R.G. (1988) Eur. J. Biochem. 180, 535–545.
[5] Pilon, M., Rietveld, A.G., Weisbeek P.J. and de Kruijff, B. (1992) J. Biol. Chem. 267, 19907–19913.
[6] Horniak, L., Pilon, M., van't Hof, R. and de Kruijff, B. (1993) FEBS Lett. 334, 241–246.
[7] Stein, M., Jacquot, J.-P. and Miginiac-Maslow, M. (1993) Plant Physiol. 102, 1349–1350.
[8] Merrifield, R.B. (1963) J. Am. Chem. Soc. 85, 2149–2154.
[9] Tam, J.P., Health, W.F. and Merrifield, R.B. (1983) J. Am. Chem. Soc. 105, 6442–6445.
[10] Girardet, J.-L., Bally, I., Arlaud, G.J. and Dupont, Y. (1993) Eur. J. Biochem. 217, 225–231.
[11] Thielens, N.M., Van Dorsselaer, A., Gagnon, J. and Arlaud G.J. (1990) J. Biol. Chem. 29, 3570–3578.
[12] Rance, M., Sørensen, O.W., Bodenhausen, G., Wagner, G., Ernst, R.R. and Wütrich, K. (1983) Biochem. Biophys. Res. Commun. 117, 479–485.
[13] Braunschweiler, L. and Ernst, R.R. (1983) J. Magn. Reson. 53, 521–528.
[14] Davis, D.G. and Bax, A. (1985) J. Am. Chem. Soc. 107, 2820–2821.
[15] Jeener, J., Meier, B.H., Bachmann, P. and Ernst, R.R. (1979) J. Chem. Phys. 71, 4546–4553.
[16] Macura, S., Hyang, Y., Suter, D. and Ernst, R.R. (1981) J. Magn. Reson. 43, 259–281.
[17] States, D.J., Haberkorn, R.A. and Ruben, D.J. (1982) J. Magn. Reson. 48, 286–292.
[18] Plateau, P. and Guéron, M. (1982) J. Am. Chem. Soc. 104, 7310–7311.
[19] Griesinger, C., Otting, G., Wüthrich, K. and Ersnt, R.R. (1988) J. Am. Chem. Soc. 110, 7870–7872.
[20] Wüthrich, K. (1986) NMR of Protein and Nucleic Acids, John Wiley, New York.
[21] Pearlman, D.A., Case, D.A., Caldwell, J.C., Seibel, G.L., Singh, U.C., Weiner, P. and Kollman, P.A. (1991) AMBER 4.0, University of California, San Fransisco, CA.
[22] Nilges, M., Clore, M. and Gronenborn, A. (1988) FEBS Lett. 239, 129–135.
[23] Brooks, C.L. and Nilsson, L. (1993) J. Am. Chem. Soc. 115, 11034–11035.
[24] Franzén, L.-G., Rochaix, J.-D. and von Heijne, G. (1990) FEBS Lett. 260, 165–168.